Use of dual-phase contrast computed tomography for evaluation of the normal canine male genital tract

H. Dirrig, R. Drees, R. Lam

Department of Clinical Sciences and Services, The Royal Veterinary College, Hertfordshire
Corresponding author email: rdrees@rvc.ac.uk

Word Count: 5702

Structured Summary

Objectives: To evaluate the use of dual-phase contrast-enhanced CT (CECT) for the depiction of the features of the male genital tract, highlighting differences between entire and neutered dogs.

Methods: CT exams of 23 entire and 23 neutered male dogs with no history of urogenital disease were included in this retrospective study, with exams acquired pre-, 30s and 98.9 +/- 27.4s post intra-venous contrast administration. The genital structures were subjectively evaluated for visibility, contrast enhancement and enhancement pattern and differences between entire and neutered dogs were described. Objective measurements of attenuation and size of the prostatic tissue were acquired.

Results: The root, body and glans of the penis could be evaluated in all dogs and appeared larger in entire dogs, though objective measurements could not be reliably made due to the curved and small nature of these structures. Contrast enhancement occurred in the cavernous structures, most reliably in the bulb and corpus spongiosum and most frequently in entire dogs in the delayed post-contrast phase. In entire dogs, the small testicular vessels most commonly had a vermiform shape in the early post-contrast phase, and a homogeneous

appearance in the delayed phase. Sternal recumbency with the coxofemoral joints extended provided superior visualisation of the genital structures.

Clinical Significance: Dual-phase CECT is useful for depiction of the structures of the male genital tract, with the early phase especially highlighting the vascular and the delayed phase the cavernous structures.

Introduction

Indications for diagnostic imaging of the canine male genital tract include evaluation of primary or secondary diseases relating to these structures, or trauma to the caudal body, including pelvic fractures, abdominal wall rupture, or perineal injury. The canine male genital structures consist of the prostate, the penis and prepuce, with the urethra contained, and in entire dogs, the scrotum, testes, epididymides, deferent ducts, spermatic cords and associated vasculature (Evans et al. 2013).

Diagnostic imaging of the male genital tract has in the past relied on a combination of standardand contrast radiography for the prostate and urethra. Transabdominal ultrasonography has been used to assess the internal architecture of the prostate (Ruel et al. 1998) as well as retained testes (Hecht et al. 2004) and direct ultrasonography is used for the normally positioned scrotal structures (England 1991, Hecht et al. 2003); both radiography and ultrasound enable measurement of the prostate (Atalan et al. 1999).

Ultrasonography, being of relative low-cost and readily available, has also been used to evaluate the penile structures in conditions such as priapism (Lavely 2009).

In human medicine, traditional diagnostic imaging modalities are often superseded by the use of the cross-sectional imaging modalities magnetic resonance imaging (MRI) (Parker et al. 2015) and computed tomography (CT) (Ali et al. 2003) for evaluation of the male genital structures. A case report of a dog with a penile injury showed that MRI was key in defining the lesion and assessing its extent, where previous radiographic and ultrasonographic examinations had been unremarkable (Hicks et al 2007). Another case report highlighted the utility of CT in diagnosing and describing a penile tumour (Furtado et al 2015).

CT has become widely available in veterinary practice and is being increasingly used for patient workup and in cases of abdominal, pelvic and hind limb evaluation, the male genital structures are routinely included in the acquired images.

Whereas the appearance of the canine prostate has already been described in healthy entire dogs (Lee et al. 2011), there are currently no studies evaluating the remainder of the canine male genital tract using dual phase contrast enhanced CT (CECT).

The aims of this study were therefore to (1) describe the CT features of the normal components of the canine genital tract in entire and neutered males, (2) evaluate the use of dual-phase CECT for the examination of these structures, (3) highlight any differences between entire and neutered males.

Materials and Methods

Patient selection

Medical records of dogs that underwent imaging of the abdomen with dual-phase CECT between January 2013 and September 2014 at our large university veterinary institution were reviewed. Male dogs without a history of urinary or genital disease and with a final diagnosis

of non-genital and non-urinary disease were selected for the study population. Urinalysis was reviewed where available and dogs with an active sediment or positive urine culture were excluded. Neutering status, including date of castration, if available, as well as breed, age and weight were noted. Entire male dogs were included even if prostatic changes consistent with benign prostatic hyperplasia (BPH) were found on examination or CT exam.

Image acquisition technique

All CT scans were acquired using a 16 multi detector row unit (Mx8000 IDT, Philips, Best, The Netherlands), the patients placed in sternal recumbency under general anaesthesia or sedation. The following scan parameters were used: helical scan mode, reconstruction slice thickness 3 mm, 1.5 mm reconstruction interval, medium frequency spatial reconstruction algorithm, 120 kVp, 100-130 mA depending on patient size, tube rotation time 2 s. In all patients, a thoracic and abdominal CT study was performed with scan direction from cranial to caudal. Pre-contrast images were obtained, and then a bolus of 2ml/kg contrast medium (Omnipaque, 300 mgl/ml, GE Healthcare AS, Nycoveie 1–2, NO-0401 Oslo, Norway) was injected through a forelimb peripheral intravenous catheterusing a power injector with up to 4 ml/s injection speed and with an upper limit of 2.24 MPa (325 PSI) injection pressure. Early and delayed phase post-contrast images were obtained 30s and 98.9 +/- 27.4 s respectively after injection of the contrast medium.

Image evaluation

Images were reviewed using commercially available viewing software (OsiriX, v.6.5.2. 64bit; Pixmeo SARL, 226 Rue de Bernex, CH1233 Bernex, Switzerland). Since patient factors such as body weight, heart rate and blood pressure were not considered for individual patients' bolus

timing, attenuation was measured in the aorta and caudal vena cava (CVC) on transverse images just cranial to the aortic branching into the internal and external iliac arteries on the early and delayed phase images, to further classify the phase of the acquired studies. The early phase post-contrast series showed predominantly arterial enhancement, with mean attenuation of the aorta of 330.7 +/- 151.9 HU and of the CVC of 94.3 +/- 55 HU. The delayed phase post-contrast series showed similar mean attenuation of the aorta (154.8 +/- 27.9 HU) and CVC (122 +/- 22.1 HU).

Position of the hind legs and visibility of the penile structures relating to the different leg positions were noted. CT exams were also evaluated for diagnostic quality and presence of any artefacts.

Structures of the prostate

The prostate was examined for visibility in all dogs. On the transverse image, it was determined if the left and right lobes of the prostate gland could be distinguished, and their respective heights were measured. Prostatic width on the transverse image ($Width_{tr}$) was defined as the maximum dimension perpendicular to prostatic height. The length of the prostate was established on dorsal plane images as the maximum distance parallel to the urethral axis for each lobe, if distinguishable. Prostatic width on the dorsal plane image ($Width_{do}$) was defined as the maximum dimension perpendicular to the longitudinal axis. Morphological features, including homogeneity and the presence of cysts or mineralisation, were recorded (noted as mineralisation yes/no, presence of cysts yes/no).

Structures of the penis

The following penile structures were evaluated for visibility (y/n), contrast enhancement (y/n for each phase), and subjective contrast enhancement pattern: extrinsic muscles of the penis (retractor penis, ischiocavernosus, bulbospongiosus, ischiourethralis); root, body and glans of the penis; urethra; os penis and prepuce. For the purpose of description, the urethra was divided into prostatic, pelvic and penile portions. The terms membranous and cavernous urethra are used in some textbooks to refer to the pelvic urethra, but for the purpose of this paper we have adhered to the most current anatomy sources (Dyce et al. 2010, Evans et al. 2013).

Pre- and post-contrast attenuation of the cavernous structures (bulb of penis, corpus cavernosum, corpus spongiosum, stratum spongiosum) were measured by drawing a circular region of interest (ROI) over the relevant areas if they could be distinguished.

Structures of the scrotum

In entire dogs, the scrotum, the testes, the epididymides and their vasculature were evaluated morphologically for visibility (y/n), contrast enhancement (y/n for each phase), and subjective contrast enhancement pattern. If the testes were homogenous, the attenuation was measured in one testicle by drawing a circular ROI on the pre, early and delayed contrast transverse images at matched locations on each phase.

The course of the spermatic cord was followed into the abdomen if possible and the position and direction of its components were noted. The diameter of the spermatic cord was measured bilaterally on transverse plane images at a point half way between the testis and the body wall. The testicular arteries and pampiniform plexus were noted if they could be seen and their appearance was described.

The following vascular structures related to the male genital organs were evaluated for visibility (y/n) and contrast enhancement (y/n for each phase): internal pudendal artery and distal branches, external pudendal artery.

Continuous data was tested for normality using the Shapiro Wilk test and if normal distribution was observed, results were presented as mean +/- standard deviation (SD). If not, they were presented as median (range). Statistical analysis was performed using a statistical software program (SPSS, version 12.0, SPSS Inc., Chicago, IL, USA).

Results

SIGNALMENT

Forty-six male dogs met the selection criteria. These included 23 entire and 23 neutered dogs. Twenty-seven different breeds were included, the most common being cross-breed (6/46), Labrador Retriever (5/46) and Jack Russell Terrier (3/46).

Final diagnosis for all dogs was recorded and included: haemangiosarcoma (4), lymphosarcoma (4), histiocytic sarcoma (3), oral and digital melanoma (3), mast cell tumour (3), undifferentiated splenic mass (2), anal sac adenocarcinoma (2), circumanal tumour (2), undifferentiated abdominal nodules/masses (2), pulmonary adenocarcinoma, nasal planum carcinoma, malignant sarcoma of the hard palate, axillary sarcoma, soft tissue sarcoma of the stifle, osteosarcoma, haemangiopericytoma, adrenal mass, steroid-responsive meningitis arteritis, immune-mediated polyarthritis, retinal detachment, glaucoma, polycythemiarubravera, hyperadrenocorticism, Sharpei fever, jejunal perforation, polyostotic

bone lesions, polymyositis, immune-mediated disease, bite wounds and faecal impaction. None of these affected the urogenital tract.

The age and body weight information of the study population is detailed in Table 1.

Urinalysis results were available for 5/23 entire and 13/23 neutered dogs. Two of the entire dogs and 7 of the neutered dogs had an inactive sediment, and the remainder had both an inactive sediment and a negative culture. The date of castration was only available in 1/23 of the neutered dogs.

POSITIONING

All dogs were placed in sternal recumbency for the CT exam. Thirty-five dogs had the coxofemoral joints extended, 8 had the coxofemoral joints flexed and 3 had the coxofemoral joints in an abducted position. This was noted to affect the visibility of the penile structures in transverse plane images specifically for the cavernous structures and the extrinsic muscles around the root of the penis; when the coxofemoral joints were in an extended position these structures were displayed elongated in the transverse plane and easy to assess. When the coxofemoral joints were flexed these structures were more difficult to distinguish as they were more curved. Hip abduction provided an intermediate ease of viewing (Fig. 1).

PROSTATE

The prostate was seen in 23/23 entire and 21/23 neutered dogs. The two prostatic lobes could be distinguished in 23/23 entire dogs but only in 5/21 of the neutered ones. Therefore, height

and length were measured individually for both left and right lobes only in the entire dogs. The internal structures of the prostate could not be distinguished in any dog or CT exam. Results of measurements of prostatic height, width ($Width_{tr}$, $Width_{do}$) and length are displayed in Table 2 and Figure 2 shows an example of three different dogs: one neutered dog where the prostate was not distinguished, a neutered dog with a small prostate and an entire dog with a larger bilobed prostate.

On pre-contrast CT images, the prostate gland was homogeneous in 9/23 entire males and in 20/21 neutered dogs in which the prostate was visible. Heterogeneity was attributed to the presence of prostatic cysts in 13/23 entire and 1/21 neutered dog, appearing as hypoattenuating, non-contrast enhancing cystic structures. Small foci of mineralisation were noted in the prostates of 2/23 entire dogs, appearing as sparse, randomly distributed dots of mineral attenuation visible in pre and post-contrast studies (Fig. 3). Only one neutered dog had heterogeneous prostatic parenchyma on pre-contrast images. This dog had been neutered one month prior and had resolving BPH which had been diagnosed as an enlarged prostate with cystic changes on a previous CT study.

Post-contrast enhancement pattern of the prostate in both early and delayed phases was heterogeneous in 23/23 entire dogs and in 4/21 neutered dogs. This was due to the presence of prostatic cysts or mineralisation in most cases, but in 10/23 entire dogs and in 3/21 neutered dogs, a specific cause could not be identified. All dogs with heterogeneous prostatic attenuation pre-contrast also had heterogeneous enhancement post-contrast. Nine (9/23) entire dogs and 3/21 neutered dogs had homogeneous prostatic attenuation pre-contrast and heterogeneous enhancement post-contrast. The timing of the contrast study (early vs delayed phase) did not affect the classification of the prostatic parenchyma as heterogeneous

or homogeneous.

PENILE MUSCULATURE, PENIS AND URETHRA

Within the root of the penis, the structures that were consistently seen in all dogs examined were the two penile crura, consisting of the two corpora cavernosa covered by the ischiocavernosus muscles, and the bulb of the penis, consisting of the bilobed spongy sacs continuous with the corpus spongiosum and covered by the bulbospongiosus muscle (Fig. 1). The retractor penis and ischiourethralis muscles were not seen on any of the CT studies.

Pre-contrast attenuation of the bulb of the penis and of the corpora cavernosa could be measured in 23/23 entire dogs and in 11/23 neutered dogs. In the remaining 12 neutered dogs, those structures were too small to accurately place a ROI for measurement. On the post-contrast studies, as described below, the structures had variable enhancement along their length and due to their small and curved shape it was not possible to reliably include the entire structure to generate an average contrast enhancement measurement. Therefore a subjective description was used for post-contrast images.

The paired corpora cavernosa were seen to originate at the ischial tuberosity. On pre-contrast exam, they appeared as soft tissue attenuating structures (53.3 +/- 9.9 HU) with a soft tissue attenuating, but slightly hyperattenuating rim, likely representing the tunica albuginea and the ischiocavernosus muscle covering the corpora cavernosa.

When it occurred (Table 3), enhancement was noted as contrast uptake near the origin of the crura with a hazy, poorly defined pattern, consistent with blood flow into the cavernous structures (Fig. 4). No contrast uptake was seen along the margins of the corpora cavernosa, presumed to be the tunica albuginea.

The bulb of the penis was seen as a widening of the tissues surrounding the caudodorsal portion of the pelvic urethra, located dorsally and medially to the two crura, dorsal to the caudal aspect of the ischial arch. The structure had a bilobed appearance and, similar to the corpus cavernosum, the centre was slightly hypoattenuating pre-contrast (mean 46.1 +/- 10.4 HU) surrounded by a more hyperattenuating rim, consistent with the surrounding fibrous layer and bulbospongiosus muscle.

Contrast enhancement of the bulb of the penis was more consistently seen compared to the corpus cavernosum (Table 3). Contrast enhancement was evident in both phases in 6/18 entire dogs. In 4 of those 6 cases, the contrast enhancement was more widespread and evident in the delayed phase, with no difference noted between phases in the other two cases.

Contrast enhancement of varying degree depending on early or late phase appeared near the origin of the bulb, between the crura, as two clearly marginated tubular structures consistent with blood flow within the bilobed arrangement of the spongy sacs (Fig. 5).

The origin of the body of the penis was seen in all dogs just caudal to the ischial arch, where the two crura joined on midline. The two corpora cavernosa remained visible as separate structures, surrounded by a slightly hyperattenuating rim, as seen in the root of the penis, however decreasing mildly in diameter as they continued distally.

Ventral to the corpora cavernosa, the corpus spongiosum could then be seen as a slightly hypoattenuating structure surrounded by a hyperattenuating rim. No distinct transition was seen between the bulb of the penis and the corpus spongiosum and this appeared as a continuous structure; the corpus spongiosum being smaller in diameter. On transverse

images the corpora cavernosa and the corpus spongiosum had an upside down Y-shape with their individual marginations visible in 19/23 entire and 9/23 neutered dogs. (Fig. 6) These structures could then be followed to the level of the caudal aspect of the os penis.

The bulbus glandis could be distinguished as a dorso-lateral bulging of the penile soft tissues at the level of the middle to caudal third of the os penis. On pre-contrast images the structure was slightly hypoattenuating with a slightly hyperattenuating rim.

The pars longa glandis was seen as a fairly homogeneous, elongated, distally tapering soft tissue-attenuating structure on pre-contrast images. In two cases, a slightly hyperattenuating structure slightly ventral to the centre, representing the urethra, was seen. Contrast enhancement of the glans was similar for the bulbus and pars longa. When present, it was irregular and patchy (Fig. 7), with no particular difference in pattern noted between the early or delayed phases.

Details of the contrast enhancement of the cavernous structures have been presented in Table 3.

The three portions of the urethra could not be clearly distinguished from the surrounding soft tissues in any of the dogs.

On transverse plane images, in the prostatic portion, a hypoattenuating V or O shape could be seen in the position of the urethra in pre-, early and delayed post-contrast images in 1/23 neutered dog (Fig. 8). This shape was also seen in the early post-contrast phase in 3/23 entire dogs, and in the delayed post-contrast phase in 8/23 entire dogs. Contrast enhancement occurred in this area in the early post-contrast phase in 13/23 entire and 1/23 neutered dogs, and in the delayed post-contrast phase in 15/23 entire and 1/23 neutered dogs. It appeared

as a ring-like pattern around the urethral position in the prostate (Fig. 9).

In the pelvic portion, a hypoattenuating V, U or O shape was also seen at times, appearing to become more O-shaped as it approached the ischial arch. This occurred in the pre-, early and delayed post-contrast images in 2/23 neutered dogs, in the early post-contrast phase in 5/23 entire dogs, and in the delayed post-contrast phase in 6/23 entire dogs.

The individual layers of the pelvic portion of the urethra, consisting of the urethra surrounded by the stratum spongiosum, urethral gland layer, tunica muscularis and urethralis muscle, could not be distinguished in any of the dogs. Pre-contrast, the structure appeared as a hypoattenuating centre with a slightly hyperattenuating rim, consistent with vascular erectile tissue surrounded by tunica muscularis and urethralis muscle, in 23/23 entire dogs and in 8/23 neutered dogs (Fig. 10A). Contrast uptake, presumably in the stratum spongiosum, appeared as a ring-like pattern around the urethra and appeared more consistently in the delayed post-contrast phase in entire dogs (Table 3, Fig. 10).

The penile portion of the urethra, surrounded by corpus spongiosum (continuous with the stratum spongiosum), could not be seen in any of the dogs on pre-contrast images. In the early post-contrast phase, only 1/23 entire dog showed contrast uptake in the corpus spongiosum, whereas in the delayed phase, this occurred in 8/23 entire dogs and in no neutered dogs (Fig. 4). Details of the contrast enhancement in the stratum and corpus spongiosum are further depicted in Table 3.

The os penis was seen as an elongated, upside-down, V-shaped mineral-attenuating structure dorsal to the urethra. The bone was completely ossified in all dogs and was not examined further.

The prepuce could be seen as a separate structure, approximately from the mid level of the os penis continuing slightly cranially to the tip of the glans penis. The structure was soft tissue-attenuating with a slightly hyperattenuating outer rim and a minimally hypoattenuating adjacent inner layer, aiding separation from the penile structures. Small spherical pockets of gas attenuation could be seen in some cases between the penis and the internal layer of the prepuce. Distinct borders of the internal and external layer of the prepuce were otherwise difficult to distinguish. The hypoattenuating fat typically seen in subcutaneous tissue was absent. No difference in the appearance post-contrast was noted.

BLOOD SUPPLY

The vessels of the penis that could be seen post-contrast in all dogs were the paired internal pudendal arteries, which could be followed to the level of the root of the penis. They were more clearly defined in the early post-contrast studies in 36/46 dogs. In 13/23 entire dogs and 11/23 neutered dogs, the arteries could be followed more distally to the paired arteries of the bulb.

The external pudendal arteries could be seen exiting at the superficial inguinal ring and supplying the prepuce in 45/46 cases, more clearly on the early studies in 36/45 dogs.

TESTICLES/SCROTUM/SPERMATIC CORD

For each individual entire dog, the left and right testicle showed similar findings. Of the 23 entire dogs, the testicles had homogeneous attenuation in all cases with pre-contrast, early and delayed post-contrast attenuations of 34.5 +/- 10.1 HU, 43.7 +/- 11 HU and 50.9 +/- 11.1

HU respectively. Internal structures such as the mediastinum testis and the testicular ligaments were not seen. The testis could be distinguished from the epididymis in 18/23 dogs. The epididymis, when seen, appeared as a semilunar soft tissue-attenuating structure along the long axis of the testis, slightly hyperattenuating to the testicular tissue with no contrast enhancement (Fig. 12). A slightly different orientation was present depending on the position of the testes and it was seen laterally, dorsally or medially adjacent to the testis. A mild widening at the caudal end of the epididymis likely represented the head of the organ.

The spermatic cord was seen in all intact dogs as a linear soft tissue-attenuating structure of 0.54 +/- 0.14 cm diameter that could be followed in the inguinal subcutaneous fat from the epididymis to the abdominal wall. Due to leg and scrotal positioning, the course of the cord outside the abdomen was not consistent and overlapping of the cord on itself or on the testis occurred at times. Intra-abdominal continuation was seen on at least one side in 20/23 cases, and could be reliably seen until separation of two linear structures occurred, presumed to be the ductus deferens and the testicular vessels (Fig. 11). Following the spermatic cord helped to localise the epididymis. The internal structures of the spermatic cord could not be differentiated on pre-contrast images. On post-contrast exams the testicular arteries showed strong contrast enhancement in the early phase in 17/23 dogs, seen as multiple interlacing vermiform lines along the length of the extra-abdominal spermatic cord (Fig. 12B). This pattern was seen solely in the early phase in 15/17 dogs and in both phases in 2/17 dogs. When this pattern was not seen, the contrast uptake along the spermatic cord was more homogeneous (Fig. 12C), most consistent with uptake in the venous plexus pampiniformis and its intermeshing with the arterial structures. This was seen in the early phase in 4/23 cases and in the late phase in 19/23 cases. The remaining 2/23 did not show visible

enhancement of the spermatic cord vessels in any of the studies.

A discontinuous contrast-enhancing rim surrounding the testes, but not the epididymis could be seen in 17/23 dogs in early phase studies and 16/23 dogs in late phase studies (Fig. 13). In 2 cases, in both phases, a thin contrast-enhancing line could be seen crossing the surface of the testis as well as around its rim. This was considered consistent with vessels taking up contrast at the surface of the testes in the tunica albuginea or visceral vaginal tunic.

Details of the contrast enhancement patterns in the structures of the entire male dogs are found in Table 4.

Similar to the prepuce, the scrotum could be differentiated as a slightly hyperattenuating change in the soft tissue attenuation of the skin. Subcutaneous fat was absent as expected. The scrotum surrounded the majority of the testis depending on its position. The scrotal septum was seen in 20/23 cases as a soft tissue-attenuating, non-contrast enhancing line extending ventrally from the penis to an ill-defined area between the testicles.

Discussion

This study is the first to describe the dual phase CECT appearance of the male genital structures. Contrast enhancement of the corpus cavernosum was not consistent nor common, but this was seen in a larger proportion of entire dogs than neutered dogs, mostly in the delayed phase. The bulb of the penis took up contrast much more reliably in entire dogs, and this was more evident in the delayed phase as well. The blood supply to the origin

of the penis has been shown to come from paired penile arteries. These initially split off into the arteries of the bulb before becoming the deep and dorsal arteries of the penis. The arteries of the bulb supply the corpus spongiosum of the bulb of the penis before anastomosing with the end branches of the deep and dorsal arteries (Evans et al. 2013). Their position as first branches off the main supplying artery may explain the superior enhancement of the bulb compared to the corpus cavernosum.

Overall, the delayed contrast phase in our dual phase studies was found to be the most useful contrast timing to observe enhancement in the cavernous structures of the penis. Delayed CECT could be helpful to evaluate the integrity of these cavernous structures especially in patients with caudal body trauma or suspected primary penile disease, most importantly in neoplasia. The use of CT in the imaging and staging of penile and prostatic cancer is routine in human medicine, with screening of at-risk patients to detect early changes a further step (Bjurlin et al. 2015, Hanyok et al. 2016, Suh et al. 2015). Having described the normal appearance of these structures in canine patients in this study will hopefully allow the abnormal to be detected more readily.

Regarding the structures in entire males, early phase studies were more likely to show a vermiform appearance in the spermatic cord, whereas a homogeneous pattern was more likely in the delayed phase. Dual phase CECT studies may be helpful to determine the exact anatomy of different structures and loss of this appearance or a marked change in size may be useful indicators of pathology in the area, such as epididymitis or testicular torsion.

There were interesting differences in the appearance of the penile structures and their contrast enhancement between entire and neutered dogs. Entire dogs showed enhancement of the cavernous structures much more commonly, and the size of the structures was subjectively larger. This was evident when trying to measure the pre-contrast attenuation of structures such as the bulb, and drawing a ROI was not possible in 12 of the 23 neutered dogs. Objective measurements of the structures for comparison was not possible due to the curved and small nature of the areas, which made reliably repeatable measurements difficult to achieve given the current methods. Contouring of the structures, 3D modeling and volume calculation would have been necessary, which was beyond the scope of this study. The neutered and entire groups were similar in terms of weight and age (Table 1) which means that neutering status could have played a part. Research has shown that androgens are responsible for the development but also the maintenance of normal penile tissue structure and function (Traish 2009). One study has found that in neutered rats, the tunica albuginea is thinner and more collagenous and the corpus cavernosum has more fibrosis and fewer smooth muscle fibres than in entire males (Shen et al 2003). This could explain why smaller structures and less contrast-enhancement were observed in the neutered dogs in this study.

In this study, the prostate was seen in all but two neutered dogs. It has been established that the prostate gland reduces in size following castration (Mahapokai et al. 2000) and large differences in size of the organ between the present study's neutered and entire dogs were indeed noted. The ability to distinguish a median septum was also much lower in neutered dogs. In entire dogs, prostate size has been shown to increase with age and in a study in Beagles, nearly all dogs over the age of 6 had changes related to BPH (Ruel et al. 1998). The CECT exams in this study were used to evaluate prostatic parenchyma and comment on its

homogeneity. A heterogeneous pattern was most common in entire dogs pre-contrast, whereas only one neutered dog had a heterogeneous prostate gland. He had been castrated very recently, and was presumably still undergoing prostatic involution. Unfortunately, the castration dates for the other neutered dogs were not available, though it was speculated that this would have been at a young age, usually between 6-12 months of age as is custom in the United Kingdom, which would explain the lack of prostatic development in these dogs. A heterogeneous pattern was attributed most commonly to the presence of cysts, which is often associated with BPH (Black et al. 1998). Histopathology would have been the next step in confirming the diagnosis of BPH but this was not performed in the present study. The results echo the findings of a prior study (Lee et al. 2011) which described the CT findings of the prostate in healthy entire dogs, with cysts being the most common cause of a heterogeneous pattern post-contrast. The prevalence of cysts was higher and the prostatic measurements were larger compared to the findings of that study and this could be attributed to the higher mean age and weight of our group of entire dogs.

In our study, the average attenuations of the prostate glands were not measured in any of the dogs. A clear distinction between the margin of the prostatic tissue and the urethra was not seen, therefore placement of a ROI was felt to be unreliable. This was especially true for the neutered cases where the prostate was smaller or not seen. Additionally, in entire cases, a majority of prostates had a heterogeneous appearance with cysts, as described above. This might have made attenuation measurement unreliable, therefore a subjective description was deemed more appropriate.

When examining the urethra, contrast enhancement was seen much more commonly in all three urethral portions of entire, compared to neutered dogs, most notably in the delayed post-contrast phase. In the prostate gland, it was impossible to determine which structure led

to the ring-like enhancement pattern seen surrounding the urethra, as the vascular tissue of the stratum spongiosum only begins caudal to the prostate (Evans et al. 2013). More caudally, contrast was taken up by the stratum spongiosum, and the pelvic urethra was the portion where the most enhancement was observed.

Anatomical reference texts describe the urethra as being U-shaped in the prostate due to the dorsally located urethral crest which remains even when the urethra is distended (Evans et al. 2013). This shape appeared only rarely, or also appeared as a V or an O. It was seen in some of the study dogs in the pelvic urethra as well, though it was noted that it became more O-shaped as it reached the ischial arch. The attenuation of the shape appeared to be identical to that of the contents of the bladder, thus most likely representing urine in the lumen of the urethra, outlining its internal surface. However, this was not considered useful enough for assessing the urethral lining.

As the dogs included in this study did not undergo post mortem examination as part of this study, future studies, including correlation of dual phase CECT with histological examinations, would be needed to further evaluate the urethral findings. Other imaging techniques may be preferable or be used in addition to CT when examining this portion of the urogenital tract, including retrograde urethrography for assessing the lumen and luminal margins and ultrasonography to evaluate the wall structure of the urethra (Ali et al. 2003, Hanson et al. 1996, Zohil et al. 1995).

Positioning of the hips had an effect on the visualisation of the structures around the penile root: positioning the coxofemoral joints in extension allowed consistently easier evaluation of the structures of the crus and bulb in the transverse plane. Position did not seem to affect

evaluation of the intra-pelvic portions or the distal penis. Considerations to positioning of a patient should be given if the study area of interest is near the ischial arch.

The orientation of the testes has traditionally been described as running in an oblique fashion, with the long axis in a dorsocaudal direction (Evans et al. 2013). Their position varied in this study, with them at times being suspended and at others in direct contact with the table at varying angles. This had an effect on the visualisation of the internal structures, including the spermatic cord, which sometimes appeared folded on itself. This was presumed to be from the orientation of the testes in the scrotum rather than an anatomical variation. This also may be taken into consideration when positioning patients for CT examination of the male genital tract by ensuring adequate space between the scrotum and the table to allow the testes to sit in a natural position.

A limitation of our study was that the contrast bolus injection parameters were not optimised for the individual patients and enhancement of the regional anatomy (Drees et al. 2014). To further characterise the position of the contrast medium in the vascular system at the given time points of the CT exams, a comparison was made between the contrast enhancement of the caudal abdominal aorta and caudal vena cava. The early phase showed predominantly arterial contrast enhancement and the delayed phase similar arterial and venous contrast enhancement, along with greater parenchymal enhancement. Future studies or exams focusing on the male urinary tract could aim to produce individually timed contrast exams to produce a distinct arterial and venous, and possibly additional parenchymal phase, likely best triggered synchronous with contrast arrival in the caudal abdominal aorta.

Due to the retrospective nature of this study, it was not possible to account and control for the many different diseases that affected the study dogs. None of the conditions were seen to grossly affect the anatomical structures that were studied. For example, the dogs with anal sac neoplasia and circumanal tumours had small, circumscribed masses which did not compress nor distort the more ventral structures. It was not possible to account for the effects of the individual patient medications or sedation and anaesthesia protocols and their impact on the imaging findings.

It was necessary to rely on historical information for the assumption that the study dogs did not have urogenital disease, and only a small number of dogs had urinalysis information available. Histopathology would have ideally been the gold standard to ensure no pathology was present in the studied structures; this was not possible in these clinical patients.

In conclusion, dual phase CECT is a valuable tool for evaluation of the canine male genital tract. Visualisation of the cavernous bodies appears best in the delayed phase in most dogs, and the structures are larger and better visualised in entire dogs compared to neutered dogs overall. The internal anatomy of certain structures such as the urethra and the testes is not well seen and examination using ultrasound or MRI may be of benefit. Future studies describing the disease features of the structures of the male genital tract using dual phase CECT would be helpful in assessing its utility in those cases.

References

Ali, M., Safriel, Y., Sclafani, S. J. A., et al. (2003) CT Signs of Urethral Injury. *Radiographics* 23, 951-963

Atalan, G., Barr, F. J., Holt, P. (1999) Comparison of ultrasonographic and radiographic measurements of canine prostate dimensions. *Veterinary Radiology and Ultrasound* 40, 408-412

Bjurlin, M. A., Rosenkrantz, A. B., Beltran, L. S. et al. (2015) Imaging and evaluation of patients with high-risk prostate cancer. *Nature Reviews Urology* 12 (11), 617-628

Black, G. M., Ling, G. V., Nyland, T. G. et al. (1998) Prevalence of Prostatic Cysts in Adult, Large-Breed Dogs. *Journal of the American Animal Hospital Association* 34, 177–80

Drees, R., Francois, C. J., Saunders, J. H. (2014) Invited review - Computed tomographic angiography (CTA) of the thoracic cardiovascular system in companion animals. *Veterinary Radiology and Ultrasound* 55, 229-240

Dyce, K. M., Sack, W. O., Wensing, C. J. G. (2010) The Male Urethra. In: Textbook of Veterinary Anatomy, 4th edn. WB Saunders, Philadelphia p 192

England, G. C. W. (1991) Relationship between ultrasonographic appearance, testicular size,

spermatozoal output and testicular lesions in the dog. *Journal of Small Animal Practice* 32, 306-311

Evans H. E., deLahunta A. (2013) The urogenital system. In: Miller's Guide to the Dissection of the dog, 4th edn. Eds H. E. Evans, A. deLahunta. WB Saunders, Philadelphia pp 368-385

Furtado, A. R. R., Parrinello, L., Merlo, M. et al. (2015) Case Report: Primary penile adenocarcinoma with concurrent hypercalcaemia of malignancy in a dog. *Journal of Small Animal Practice* 56, 289-292

Hanson, J. A., Tidwell, A.S. (1996) Ultrasonographic appearance of urethral transitional cell carcinoma in ten dogs. *Veterinary Radiology and Ultrasound* 37, 293-299

Hanyok, B. T., Howard, L. E., Amling, C. L. et al. (2016) Is computed tomography a necessary part of a metastatic evaluation for castration-resistant prostate cancer? Results from the Shared Equal Access Regional Cancer Hospital Database. *Cancer* 122 (2), 222-229

Hecht, S., Matiasek, K., Kostlin, R. (2003) Scrotal sonography in the dog with a focus on testicular neoplasia. *Tierarztliche Praxis* 31 Iss.4, 199-210

Hecht, S., King, R., Tidwell, A. S. et al. (2004) Ultrasound diagnosis: intra-abdominal torsion of a non-neoplastic testicle in a cryptorchid dog. *Veterinary Radiology and Ultrasound* 45, 58-61

Hicks, D. G., Bagley, R. S., Gavin, P. R., et al. (2007) Imaging diagnosis - Corpus cavernosum, ischiocavernosus and bulbospongiosus muscle injury in a dog. *Veterinary Radiology and Ultrasound* 48, 239-242

Lavely, J.A. (2009) Priapism in dogs. *Topics in Companion Animal Medicine* 24, 49-54

Parker III, R.A., Menias, C.O., Quazi, R., et al. (2015) MR Imaging of the Penis and Scrotum. *Radiographics* 35, 1-18

Lee, K-J., Shimizu, J., Kishimoto, M., et al. (2011) Computed tomography of the prostate gland in apparently healthy entire dogs. *Journal of Small Animal Practice* 52, 146-151

Mahapokai, W., Xue, Y., van Garderen, E. et al. (2000) Cell Kinetics and Differentiation after Hormonal-Induced Prostatic Hyperplasia in the Dog. *The Prostate* 44, 40-48

Ruel, Y., Barthez, P.Y., Mailles, A., Begon, D. (1998) Ultrasonographic evaluation of the prostate in healthy intact dogs. *Veterinary Radiology and Ultrasound* 39, 212-216

Shen, Z-J., Zhou, X-L., Lu, Y-L. et al. (2003) Effect of Androgen Deprivation on Penile Ultrastructure. *Asian Journal of Andrology* 5, 33-36

Suh, C. H., Baheti, A. D., Tirumani, S. H. et al. (2015) Multimodality imaging of penile cancer: what radiologists need to know. *Abdominal Imaging* 40 (2), 424-435

Traish, A. M. (2009) Androgens Play a Pivotal Role in Maintaining Penile Tissue Architecture and Erection: A Review. *Journal of Andrology* 30, 363-369

Zohil, A. M., Castellano, M.C. (199) Prepubic and transrectal ultrasonography of the canine prostate: a comparative study. *Veterinary Radiology and Ultrasound* 36, 393-396

Tables:

Table 1: Age and Weight of the Study Dogs* According to Neutering Status

	Median		Mean (SD†)		Minimum-Maximum	
	Entire	Neutered	Entire	Neutered	Entire	Neutered
Age (years)	9.9	8.8	8.7 (3.5)	8.8 (3.1)	1.1-15	3.2-14.2
Weight (kg)	24	24	25.9 (14.5)	24.7 (11.2)	8.1-56.8	7-47

*Entire n = 23. Neutered n = 23. †SD: Standard Deviation.

Table 2: Prostatic Dimensions for the Study Dogs*

	Mean (SD†)		Minimum-Maximum	
	Entire	Neutered	Entire	Neutered
Height (cm)	Left lobe: 3.2 (0.8)	1.2 (0.4)	1.7-5.2	0.7-2.1
	Right lobe: 3.1 (0.8)‡			
$Width_{tr}$§ (cm)	4.0 (0.9)	1.5 (0.7)	2.5-5.7	0.8-4.2
Length (cm)	Left lobe: 3.3 (0.9)	2.0 (0.7)	1.6-5.1	0.9-4.6

	Right lobe: 3.4 (0.9)‡			
$Width_{do}$[‖] (cm)	4.1 (0.9)	1.4 (0.7)	2.5-5.8	0.8-4.3

*Entire n = 23. Neutered n = 23.†SD: Standard Deviation.‡The two prostatic lobes were measured individually only in entire dogs as they could only be distinguished in 5/21 neutered dogs. [§]$Width_{tr}$: width in the transverse plane; [‖]$Width_{do}$: width in the dorsal plane.

Table 3: Contrast Enhancement Characteristics of Cavernous Structures in the Study Dogs*

	Contrast enhancement in early phase		Contrast enhancement in delayed phase		No contrast enhancement in either phase	
	Entire	Neutered	Entire	Neutered	Entire	Neutered
Stratum spongiosum	13 (57%)	1 (4%)	21 (94%)	4 (17%)	2 (9%)	19 (83%)
Corpora cavernosa	3 (13%)	0 (0%)	4 (17%)	2 (9%)	19 (83%)	21 (91%)
Bulbus penis	6 (26%)	0 (0%)	18 (78%)	7 (30%)	5 (22%)	16 (70%)
Corpus spongiosum	1 (4%)	0 (0%)	8 (35%)	0 (0%)	15 (65%)	23 (100%)
Bulbusglandis	5 (22%)	0 (0%)	5 (22%)	0 (0%)	18 (78%)	23 (100%)

*Entire n = 23. Neutered n = 23.

Table 4: Contrast Enhancement Patterns of the Spermatic Cord and Testicle in the Entire Male Dogs (n=23)

	Contrast enhancement	Contrast enhancement	No enhancement in

	early phase	delayed phase	either phase
Spermatic cord appearance	Vermiform: 17 (74%) Homogenous: 4 (17%)	Vermiform: 2 (9%) Homogenous: 19 (83%)	2 (9%)
Contrast enhancing rim around testes	17 (74%)	16 (70%)	6 (26%)

Figure legends:

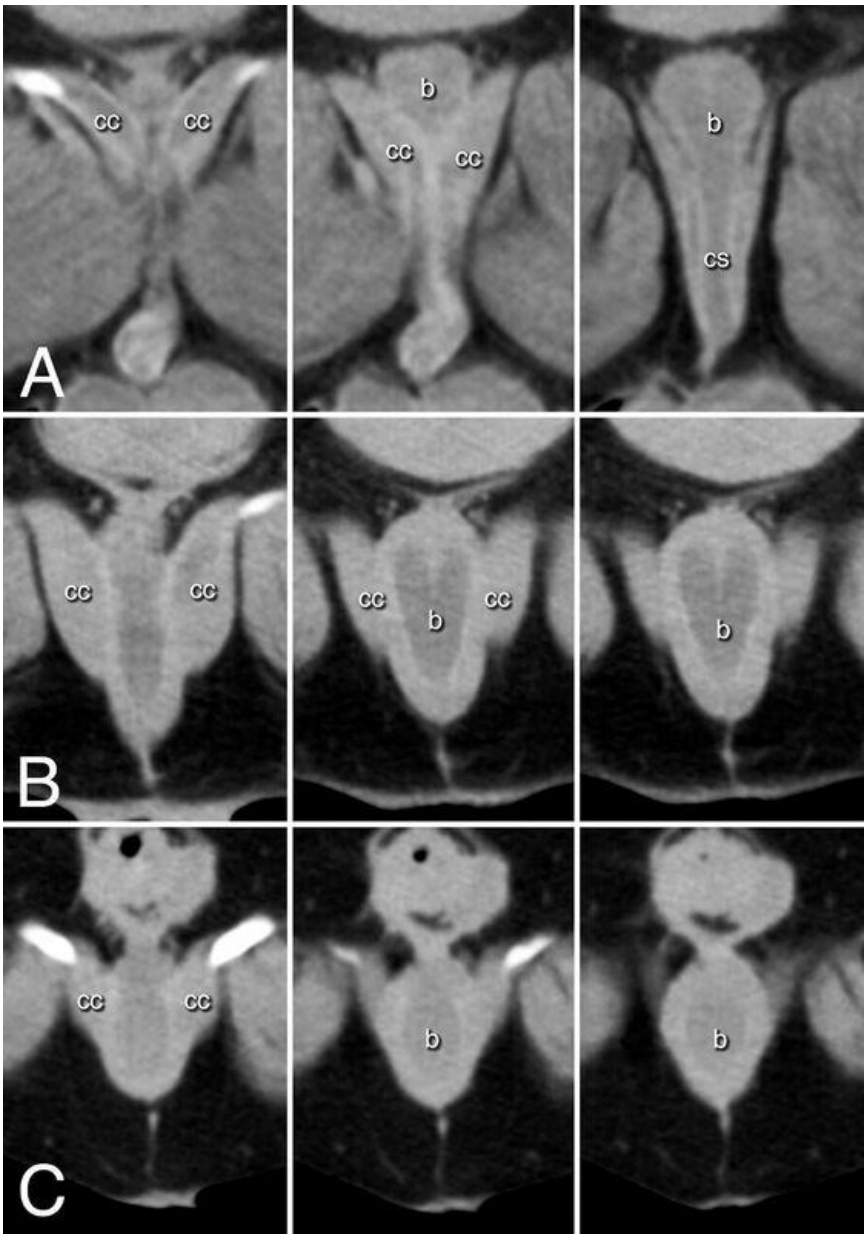

Figure 1: Impact of leg positioning on visibility of the penile structures shown in consecutive pre-contrast CT images of three different dogs, displayed from cranial (left) to caudal (right). A: entire dog with coxofemoral joints in extended position, showing elongation of the extrinsic muscles of the penis. B: entire dog with coxofemoral joints abducted. C: neutered dog with coxofemoral joints flexed; both positions (B, C) showing shortening of the cavernous structures (b: bulbus penis, cc: corpus cavernosum, cs: corpus spongiosum).

Figure 2: Pre-contrast CT images of the prostate of three different dogs. A: neutered dog where the prostate was not distinguished along the urethra (arrow) caudal to the bladder neck. B: neutered dog where the prostate could be distinguished as a bulge around the urethra but without distinct lobes (arrow-head). C: entire dog where the prostate appeared as a bilobed structure (arrow-head).

Figure 3: CT image of the prostate of two different entire dogs. A: pre-contrast administration, showing prostatic mineralisation (arrows). B: after contrast administration, showing a heterogeneous prostate gland and a prostatic cyst (arrow-head).

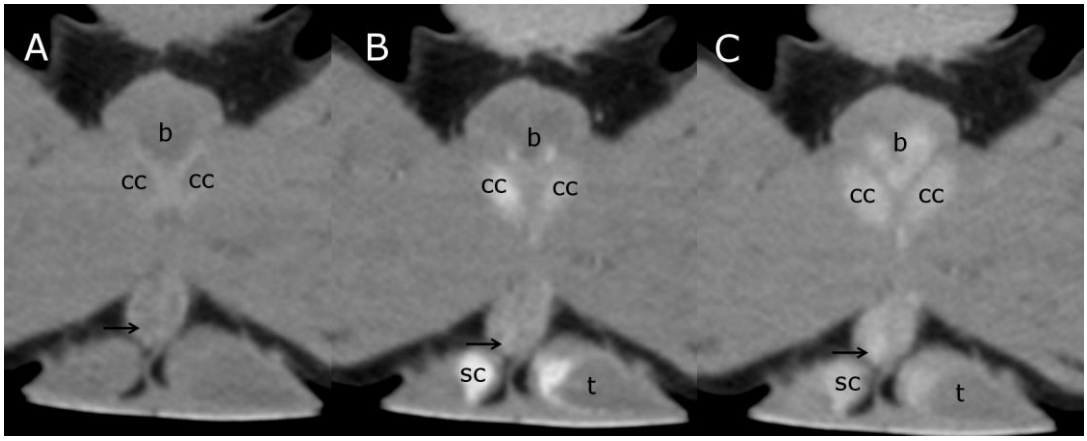

Figure 4: CT images of an entire dog showing pre-contrast (A), early (B) and delayed (C) post-contrast images of the root of the penis. In the post-contrast phases there is contrast uptake in the bilobed bulb (b) but also in both corpora cavernosa (cc), more widespread in the delayed study. More ventrally, there is also contrast uptake in the corpus spongiosum (arrows) surrounding the urethra in the penis, and in the spermatic cord (sc) vessels, showing a homogeneous pattern of uptake. (t=testis)

Figure 5: CT images of an entire dog showing pre-contrast (A), early (B) and delayed (C) post-contrast images of the penile root, showing the bulb of the penis (b) and its continuation as the corpus spongiosum (cs). There is superior enhancement of the bulb of the penis in the delayed study and its bilobed arrangement can be seen.

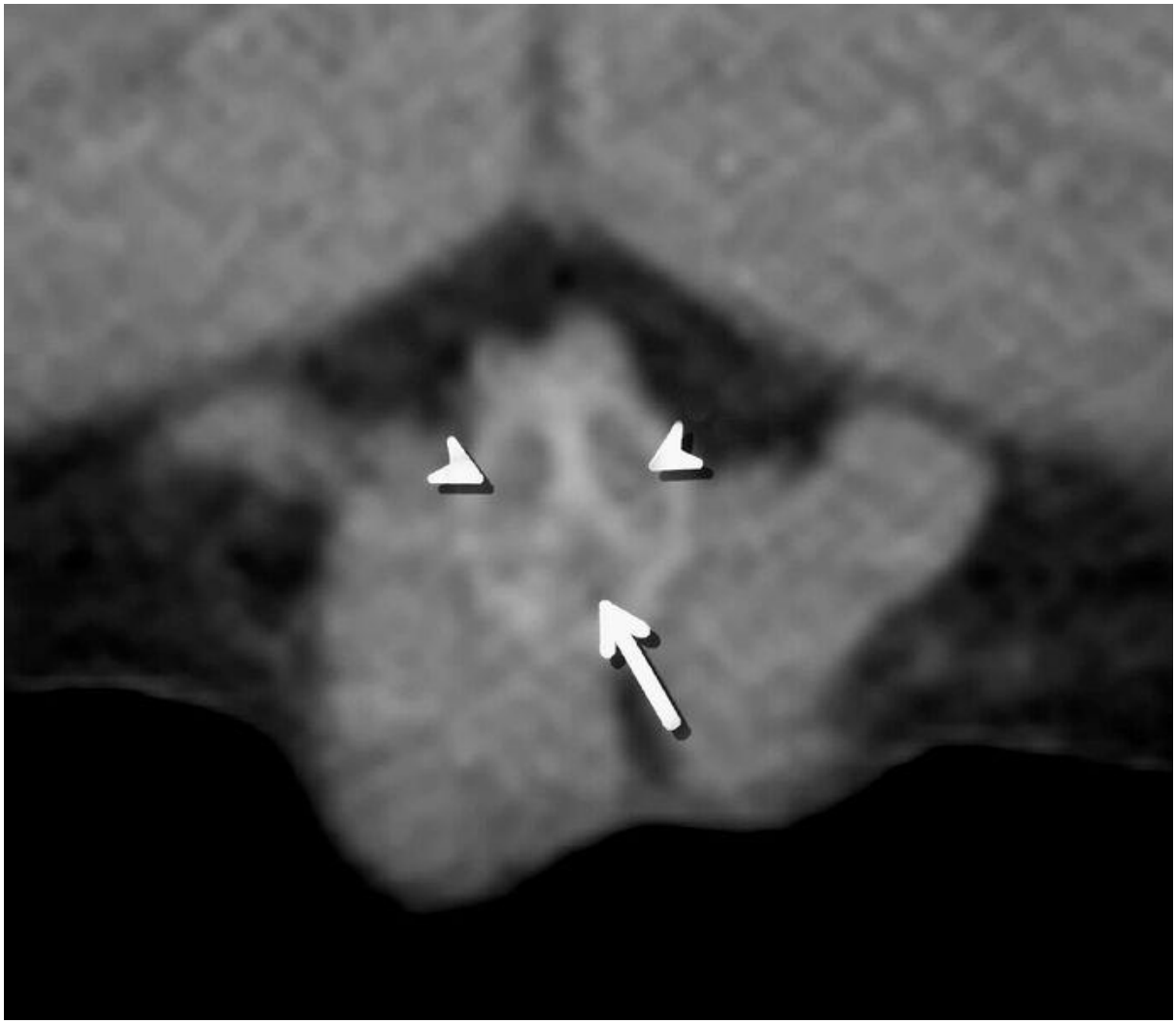

Figure 6: Pre-contrast CT image of the penis showing the bilateral corpora cavernosa (arrowheads) and the corpus spongiosum (arrow) clearly separated by an inverted hyperattenuating Y-shaped structure.

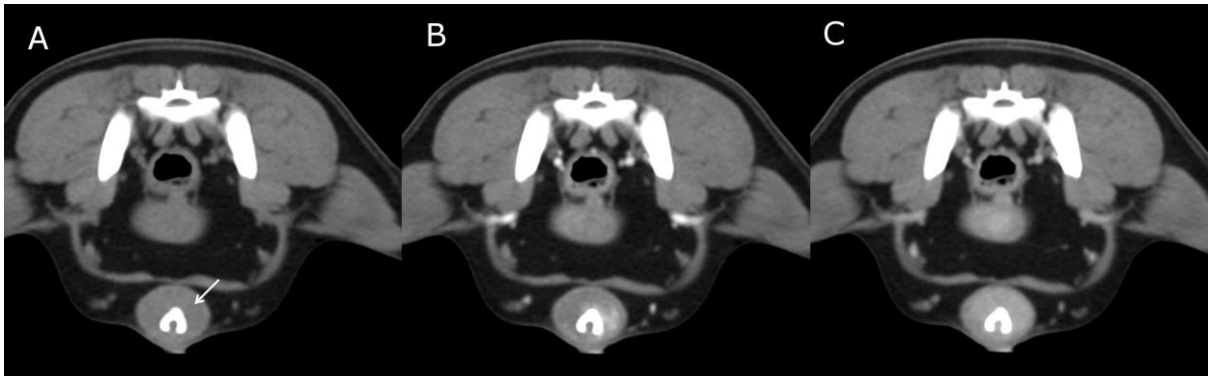

Figure 7: Pre-contrast (A), early (B) and delayed (C) post-contrast CT images of the bulbus glandis (arrow) of an entire dog, showing the patchy, unpredictable contrast enhancement pattern, in this case appearing more homogeneous in the delayed post-contrast phase.

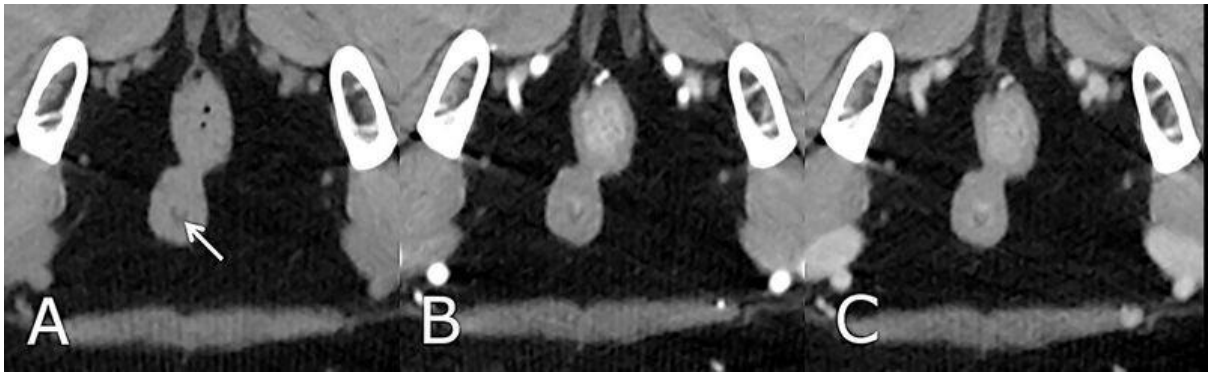

Figure 8: CT study showing pre-contrast (A), early (B) and delayed (C) post-contrast images of the prostatic urethra of a neutered dog. The V shape (arrow) is visible in all images and there is some contrast uptake around the area in both the early and delayed post-contrast images.

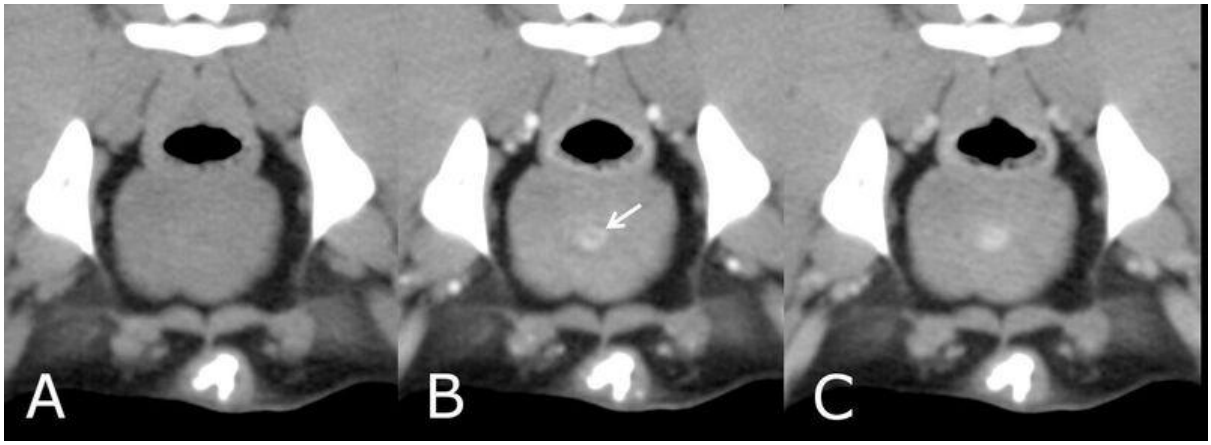

Figure 9: CT study showing pre-contrast (A), early (B) and delayed (C) post-contrast images of the prostatic urethral area of an entire dog. In this case, there is contrast uptake in a ring around the area of the urethra (arrow) in both post-contrast studies.

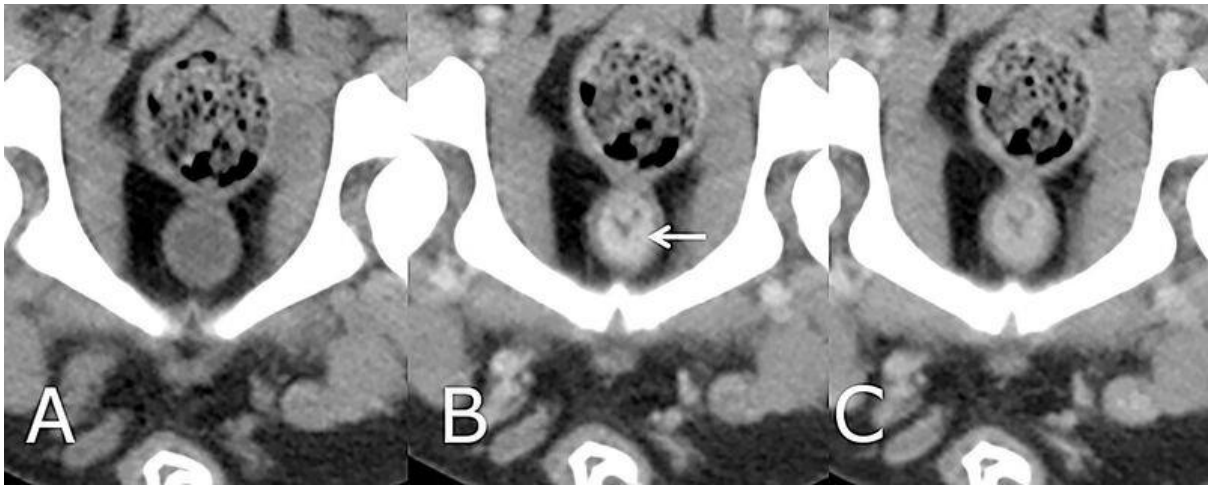

Figure 10: CT study of an entire dog showing pre-contrast (A), early (B) and delayed (C) post-contrast images of the pelvic urethral area. The hypoattenuating V shape is evident in the post-contrast images, surrounded by an area of increased contrast uptake, consistent with the stratum spongiosum (arrow).

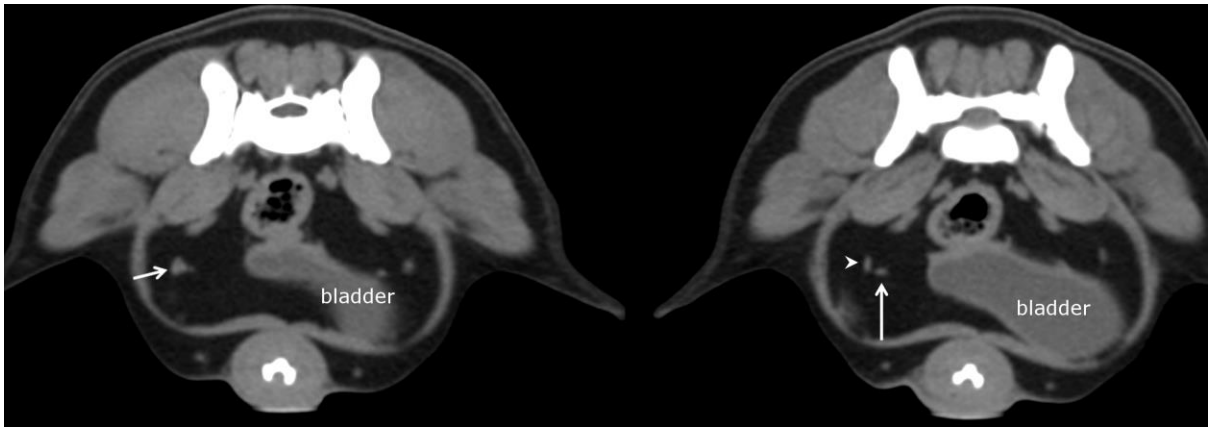

Figure 11: Two consecutive CT images from the same study of an entire dog, showing the right intra-abdominal spermatic cord (short arrow) and its separation into the testicular vessels (arrowhead) and ductus deferens (long arrow).

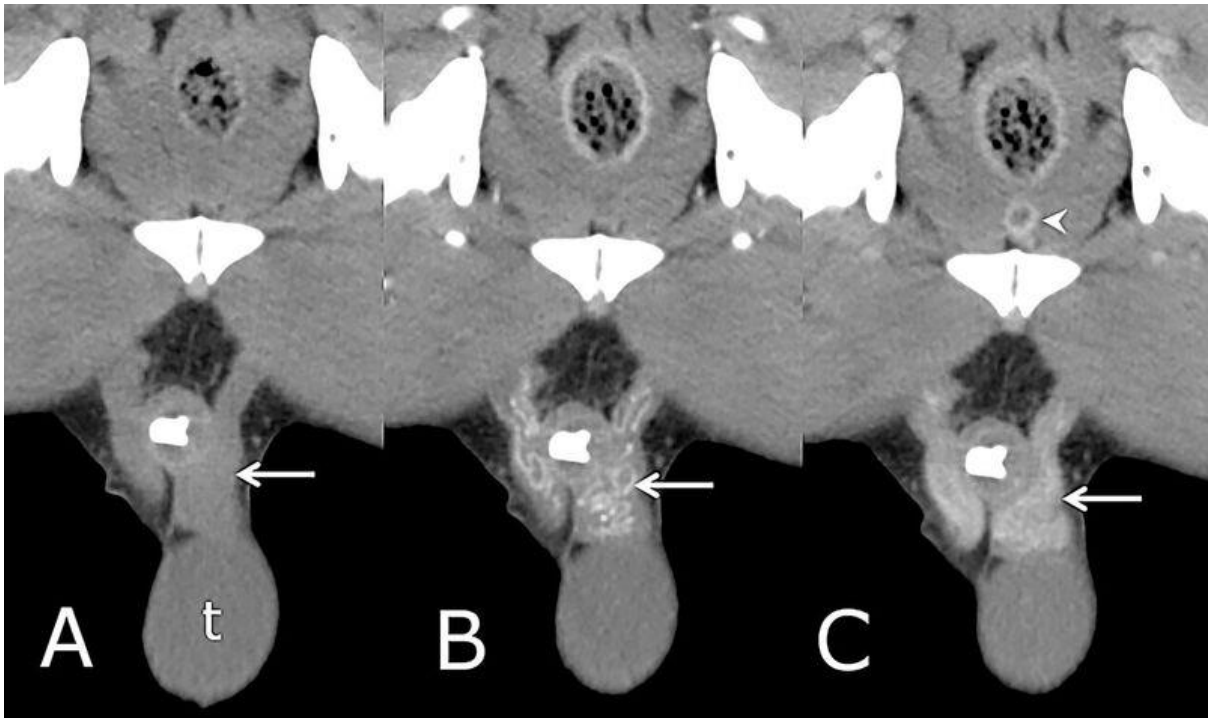

Figure 12: Pre-contrast (A), early (B) and delayed (C) post-contrast images of an entire dog, showing the enhancement pattern of the extra-abdominal spermatic cord (arrows). The vermiform appearance of the spermatic cord is evident in the early post contrast phase, whereas the enhancement is more homogeneous in the delayed post contrast phase. On the delayed post-contrast image contrast enhancement around the urethra is seen distinctly in this dog (arrowhead). (t=testis)

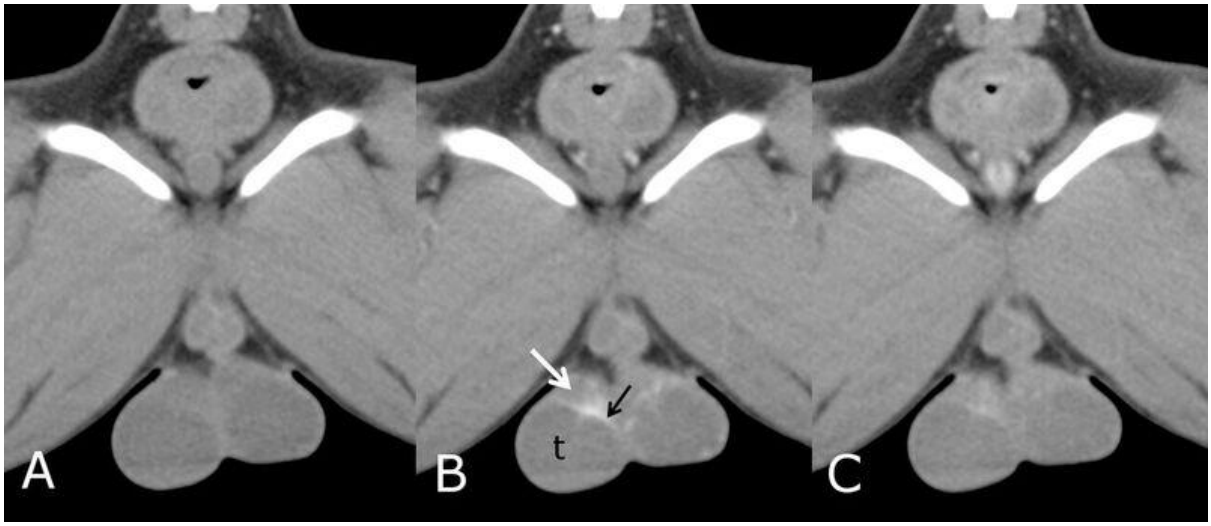

Figure 13: CT study of pre-contrast (A), early (B) and delayed (C) post-contrast images of an entire dog showing a contrast-enhancing rim (black arrow) around the testes (t), most distinct in the early post contrast phase. This contrast enhancing rim does not surround the epididymis (white arrow).